PERGAMON

International Journal of Solids and Structures 38 (2001) 4797–4823

INTERNATIONAL JOURNAL OF SOLIDS and STRUCTURES

www.elsevier.com/locate/ijsolstr

Self-intersection in elasticity

Adair Aguiar [a], Roger Fosdick [b,*]

[a] *Department of Mechanical Engineering and Materials Science, MS 321, Rice University, Houston, TX 77251 1892, USA*
[b] *Department of Aerospace Engineering and Mechanics, University of Minnesota, 107, Akerman Hall, 110, Union Street S.E., Minneapolis, MN 55455, USA*

Received 20 October 1999; in revised form 9 August 2000

Abstract

This study represents a contribution to the local behavior of the solutions of the governing equations of elastostatics in the vicinity of corners. It contains an asymptotic investigation – within both the linear and two special nonlinear theories of plane strain – of the deformation field near a corner point that separates a free and a fixed part of the boundary. Our computations confirm that the asymptotic solutions represent the local behaviors of equilibrium states very close to the corner. In this neighborhood the linear and nonlinear theories predict very different behavior. Away from the corner the deformation gradient becomes small and the asymptotic solution in the nonlinear theory becomes – expectedly – not valid. However, in an intermediate region our numerical results obtained from both the linear and nonlinear theories show striking similarities and predict a novel behavior of the free surface.

Keywords: Asymptotic; Bonded; Contact; Nonlinear elasticity; Plane strain; Punch; Self-intersection; Singularities; FEM

1. Introduction

In classical linear elastostatics, a solution of the governing equations can have serious irregularities at the boundary of a domain. In particular, the displacement gradient field can be singular at boundaries containing corners. Such singularities are outside the range of application of the theory because they contradict the assumption of small gradients upon which the theory is founded. Nevertheless, the study of the linear theory reveals some interesting aspects that can be used in the study of the asymptotic behavior of solutions in certain nonlinear theories.

The displacement field u in plane linear elastostatics has the asymptotic expansion

$$u(R,\Theta) \approx \sum_{\Re b_j>0} \sum_{k=0}^{k_j-1} R^{b_j} \log^k R v_{jk}(\Theta) \tag{1}$$

* Corresponding author. Fax: +1-612-626-1558.
E-mail address: fosdick@aem.umn.edu (R. Fosdick).

0020-7683/01/$ - see front matter
PII: S0020-7683(00)00325-5

in the vicinity of a corner, where (R,Θ) are the polar coordinates with origin at the corner, v_{jk} are infinitely differentiable complex functions, and b_j are complex roots with multiplicity k_j of a transcendental equation $\Delta(b_j)=0$. The works of Kondrat'ev (1967), Kondrat'ev and Oleinik (1983), Grisvard (1985, 1986, 1992), Dauge (1988), and Leguillon and Sanchez-Palência (1987) are standard references in this area. At a corner where homogeneous traction and displacement boundary conditions are prescribed on adjacent sides, the transcendental equation is of the form

$$\Delta(b)\equiv\begin{cases}-(1+\kappa^2)-2\kappa\cos(2\alpha b)+2(1-\cos(2\alpha))b^2 & \text{if } \alpha\neq\pi,\\ \kappa-e^{2i\pi(b-1/2)} & \text{if } \alpha=\pi,\end{cases}\tag{2}$$

where κ is a material constant, $1<\kappa<3$, and α is the angle of the corner. This expression is well-known in the literature and has been studied by Bogy (1971) and Reitich (1991). Clearly, if $\Re b<1$, the gradient of the displacement field is unbounded at the origin, which limits the applicability of the classical linear theory. Also, if $\Im b\neq 0$ then infinite oscillations of the form $\cos(\Im b\log r)$ and $\sin(\Im b\log r)$ are predicted in the vicinity of the corner.

Singularities of the oscillatory type in the stress field at a crack tip have been known for years and were reported by Williams (1959) and Rice and Sih (1965) in their investigations of half-planes of dissimilar materials bonded over portions of their common boundary. Also, Knowles and Sternberg (1975,1977) (and authors cited therein) investigated the anomalous oscillatory behavior in two classical singular problems of elasticity theory. The self-intersection of matter found in one of these problems and the change of sign of the contact force found in the other, caused them to conclude that these problems have no solution within the conventional linear setting. They then showed that for a particular class of nonlinear elastic materials the anomalous behavior, which is related to a spurious self-intersection anomaly, could be resolved. We comment more on their approach later in this section.

In an attempt to resolve the overlapping of material at the crack interface that divides two different isotropic, homogeneous linear elastic bodies that occupy complementary semi-infinite half-spaces in $\mathbb{R}^2$, Comninou (1977,1978) and Comninou and Schmueser (1979) imposed the *closed crack tip* condition, i.e., the condition that the deformed crack faces remain in contact in a neighborhood of the crack tips. Their computations showed the existence of two contact zones, one at each tip, the length of which depended very strongly on the remotely applied loading conditions. Later, Aravas and Sharma (1991) questioned this work and showed that when one of the half-spaces is rigid the asymptotic solution based on the closed crack tip condition predicts self-intersection, contrary to the work of Comninou et al. They observed that if the length of the contact zone is small compared to the crack length, the traditional solution, which is based on the assumption of traction-free crack faces and does not employ the closed crack tip condition, is still valid over distances that are larger than the contact zone size but still small compared to the crack length.

Our goal in this paper is to use a representative nonlinear theory of elasticity to gain understanding of the behavior of the deformation field in the vicinity of points on the boundary of an elastic body where the boundary conditions are not smooth. In particular, stress-displacement boundary conditions are imposed along the straight boundary of the half-plane. Our previous work, Aguiar and Fosdick (2000), represents a starting point toward this end. In that work we introduced a computational framework for the investigation of the corner behavior of solutions to plane problems in *incompressible nonlinear elasticity theory*. Our idea was to use a one-parameter family of compressible elastic materials so that, both, the constitutive relation reduces to that of a given incompressible material and the constraint of incompressibility is recovered as the parameter tends to zero. Our finite element method was based on the classical *Galerkin formulation* and it used a *continuation technique* that is based on the Newton–Raphson procedure. This employed the idea of an arc length continuation in order to construct a one-parameter continuous path of states through the solution of a nonlinear problem, starting from a known solution to a more elementary problem. We shall apply that idea here as well.

In our earlier work we studied the behavior of the deformation field near the corner of a polygonal domain, where a singularity is likely but not certain. We concentrated on the corner behavior of the *compressed bonded block problem*, i.e., the large axial compression of an incompressible, isotropic, elastic block with free sides and clamped ends. We argued that the deformed free surface does not have a monotonicaly increasing bulge in the vicinity of the corners of the block, but does so only away from the corners in relation to the overall widening of the block. The coupling of the local constraint of volume preservation together with the behavior of the deformation field near the corner gave rise to numerical errors that very much complicated our work. Even though the numerical issues associated with the constraint of incompressibility have been satisfactorily resolved within the context of the classical linear theory, it is still unclear how to accurately impose this restriction within the context of the nonlinear theory. In the present work we relax the constraint of incompressibility and continue the study of the corner behavior within the context of a representative *compressible nonlinear elasticity* theory.

Although several different nonlinear constitutive relations were considered during the course of this investigation, we concentrate here on the particular class of *harmonic materials*. This class was introduced by John (1960) and has been used by others, among which we cite Knowles and Sternberg (1975,1977), Ogden (1977), Isherwood and Ogden (1977), Carroll (1988), and Steigmann and Pipkin (1988), in their studies of the nonlinear theory. We analyze the *bonded punch problem* for a subclass of harmonic materials and compare our results to those from the classical linear theory. Here, by the bonded punch problem we mean the plane-strain problem for a half-plane which arises by requiring that a finite segment of the boundary undergo a constant rigid normal translation by means of an axially loaded, bonded flat-ended rigid punch. The remainder of the boundary, as well as the points at infinity, are supposed to be free of traction in such a way that the half-plane is in equilibrium. The subclass of harmonic materials that we adopt has the asymptotic constitutive structure proposed by Knowles and Sternberg (1975) when the sum of the principal stretches, ω_1, tends to infinity. This asymptotic structure implies that a rectangular piece of the material subject to homogeneous uni-axial tension maintains a nonzero width for any finite but arbitrarily large uni-axial stretch. Otherwise, our response function follows the behavior of the *semi-linear material*, which was also introduced by John (1960). For this reason, we refer to our response function as *modified semi-linear*. While John's semi-linear material has a very simple constitutive structure that makes it attractive for theoretical analysis and numerical computations, it yields deformation fields with spurious oscillatory behavior in the vicinity of corners. Thus, we use it in this work only for comparison purposes with the modified semi-linear material when ω_1 is not large.

We are particularly interested in the behavior of solutions in the neighborhood of the corners of the bonded punch. To study this, we employ the asymptotic analysis of Knowles and Sternberg (1975) in their investigation of the bonded punch problem. We then present asymptotic expressions which do not have spurious oscillations and which preclude the possibility of both self-intersection and local eversion of material in the vicinity of the corners of the punch. We use these expressions to predict the free surface behavior and we provide independent finite element computations which confirm these predictions and determine the interior behaviors as well. We also present analogous asymptotic expressions obtained from the investigation of the bonded punch problem within both the classical linear and semi-linear theories. These expressions predict spurious oscillations for the deformation field and are used here to illustrate the limitations of these theories. In addition, since the closed form solution for the linear theory is well-known and can be found in the classical literature (e.g., Milne-Thomson, 1968; Muskhelishvili, 1963), we use the solution of the linear problem to check and authenticate our computational scheme in the vicinity of the corners of the punch.

The asymptotic and computational analyses reveal the existence of three regions with different characteristic behaviors in both the linear and nonlinear (semi-linear and modified semi-linear) theories. Very close to the corners, we identify a *singular region* for which the stress field has a square-root singularity and both the linear and the semi-linear materials predict self-intersection and local eversion of material. No such anomalous behavior is predicted by the modified semi-linear material. Also, the deformed free surface

profiles are very different in this region. As we move away from the corners, we identify an *intermediate region* of lower gradients of deformation for which both theories predict a novel, but physically possible, behavior of the corresponding deformed free surfaces. Far away from the corners, we identify a *far-away region* for which the deformed free surface profiles become parallel. In particular, these surfaces are indistinguishable in the semi-linear and modified semi-linear cases.

In summary, in Section 2 we present preliminary developments that are useful throughout the paper. In Section 3 we present constitutive inequalities that are essential in order for the general harmonic material to be physically sensible. In Section 4 we present the mathematical formulation of the bonded punch problem for the modified semi-linear material and we investigate the asymptotic behavior of the solution to this problem in the vicinity of the corners of the punch. In Section 5 we display graphically our predictions within both the linear and nonlinear theories, and illustrate that our asymptotic and computational results are in very good agreement in the vicinity of the corners of the punch. In Section 6 we present some concluding remarks.

2. Preliminaries

In this work we consider the planar deformation of an isotropic elastic body. We suppose that the reference configuration of the body is an open, bounded set $\mathbb{B} \in \mathbb{R}^2$, and the particles $\mathbf{X} \in \mathbb{B}$ are defined by their coordinates $\mathbf{X} = (X_1, X_2)$ relative to a fixed orthonormal basis $\{\mathbf{i}_1, \mathbf{i}_2\}$. This reference configuration is assumed to be an undistorted and stress-free natural state. The *deformation* of $\mathbb{B}$ is a smooth map $\mathbf{y}$: $\mathbb{B} \to \mathbb{R}^2$, and we let $\mathbf{x} = \mathbf{y}(\mathbf{X})$ be the deformed position of the particle $\mathbf{X}$. The coordinates of $\mathbf{x} = (x_1, x_2)$ are also relative to the basis $\{\mathbf{i}_1, \mathbf{i}_2\}$. *The deformation gradient* is given by $\mathbf{F} = \nabla \mathbf{y}$.

For a compressible, isotropic elastic body, the *Cauchy stress* is given by the constitutive relation (see Fosdick and Schuler, 1969),

$$\mathbf{T} = \frac{\partial W}{\partial J}\mathbf{1} + \frac{2}{J}\frac{\partial W}{\partial I}\mathbf{B}, \tag{3}$$

where $\mathbf{B} = \mathbf{F}\mathbf{F}^{\mathrm{T}}$, $I = \operatorname{tr}\mathbf{B} = |\mathbf{F}|^2$, $J = \det \mathbf{F}$, and $W = W(I, J)$ is the *strain energy function* per unit reference area. Because the reference configuration $\mathbb{B}$ is a natural state we know that $W(\cdot,\cdot)$ must satisfy

$$\frac{\partial W}{\partial J}(2,1) + 2\frac{\partial W}{\partial I}(2,1) = 0. \tag{4}$$

The *Piola–Kirchhoff* stress is defined by

$$\mathbf{S} \equiv (\det \mathbf{F})\mathbf{T}\mathbf{F}^{-\mathrm{T}} = \mathbf{T}\operatorname{cof}\mathbf{F}. \tag{5}$$

One of the advantages of introducing this tensor is that the equation of equilibrium, in the absence of body forces, can then be expressed as a differential equation in the reference configuration, i.e.,

$$\operatorname{Div}\mathbf{S}(\mathbf{X}) = 0, \quad \mathbf{X} \in \mathbb{B}. \tag{6}$$

Now, given a strain energy function, the *mixed problem of elastostatics* consists of finding a deformation field $\mathbf{y} : \mathbb{B} \to \mathbb{R}^2$ whose stress field of Eqs. (3) and (5) satisfies the equation of equilibrium (6) subject to the boundary conditions

$$\mathbf{y}(\mathbf{X}) = \bar{\mathbf{y}}(\mathbf{X}), \qquad \mathbf{X} \in \Gamma_y, \tag{7}$$

$$\mathbf{S}(\mathbf{X})\mathbf{m}(\mathbf{X}) = \bar{\mathbf{s}}(\mathbf{X}), \quad \mathbf{X} \in \Gamma_s, \tag{8}$$

where the boundary of $\mathbb{B}$ is decomposed according to $\partial\mathbb{B} = \Gamma_y \cup \Gamma_s$, $\overset{\circ}{\Gamma}_y \cap \overset{\circ}{\Gamma}_s = \emptyset$, and $\mathbf{m}(\cdot)$ is the outer unit normal field to $\mathbb{B}$. If $\Gamma_y = \emptyset$ then the given traction field $\bar{\mathbf{s}}$ must satisfy the usual global equilibrium con-

dition that is essential for the existence of a solution. Using Eqs. (3) and (5), we find that the Piola–Kirchhoff stress $\mathbf{S}$ has the reduced form

$$\mathbf{S} = \frac{\partial W}{\partial J}\operatorname{cof}\mathbf{F} + 2\frac{\partial W}{\partial I}\mathbf{F}. \tag{9}$$

It will be convenient later to replace I and J by the auxiliary invariants ω_1 and ω_2, both positive and defined by

$$\begin{aligned} \omega_1^2 &\equiv I + 2J, \\ \omega_2^2 &\equiv I - 2J. \end{aligned} \tag{10}$$

Then, Eq. (9) has the form

$$\mathbf{S} = (\mathbf{F} + \operatorname{cof}\mathbf{F})\Phi_{\omega 1} + (\mathbf{F} - \operatorname{cof}\mathbf{F})\Phi_{\omega_2}, \tag{11}$$

where

$$\Phi_{\omega\alpha}(\omega_1, \omega_2) = \frac{1}{\omega_\alpha}\frac{\partial W(I(\omega_1, \omega_2), J(\omega_1, \omega_2))}{\partial \omega_\alpha}, \tag{12}$$

($\alpha = 1$ or 2, not summed). It is then easy to see that Eq. (6) has the form

$$(\mathbf{F} + \operatorname{cof}\mathbf{F})\nabla\Phi_{\omega_1} + (\mathbf{F}\operatorname{cof}\mathbf{F})\nabla\Phi_{\omega_2} + (\Phi_{\omega_1} + \Phi_{\omega_2})\operatorname{Div}\mathbf{F} = 0. \tag{13}$$

In the reference configuration, $(\omega_1, \omega_2) = (2,0)$, and we shall set

$$\Phi_{\omega_1}(2,0) = 0, \qquad \frac{\partial(\omega_1\Phi_{\omega_1})}{\partial\omega_1}(2,0) = \lambda + \mu, \qquad \Phi_{\omega_2}(2,0) = \mu. \tag{14a, b, c}$$

The condition (14a) is a consequence of Eq. (4) while the conditions (14b,c) ensure that the strain energy density reduces to the classical quadratic form for infinitesimal theory. The constants λ and μ are the Lamé constants of the linear theory, and they satisfy the classical inequalities

$$\mu > 0, \qquad \lambda + \mu > 0. \tag{15}$$

A *harmonic material* is characterized by the assumption that $\Phi_{\omega_2} = \text{constant}$ (John, 1960), and in this case the strain energy density has the form

$$W(\omega_1, \omega_2) = 2\mu[\phi(\omega_1) - J(\omega_1, \omega_2)], \tag{16}$$

where ϕ is a smooth function and, from Eq. (10), $J(\omega_1, \omega_2) = (\omega_1^2 - \omega_2^2)/4$. Of course, Eq. (14c) is trivially satisfied and we observe from Eq. (12) that

$$\Phi_{\omega_1}(\omega_1, \omega_2) = \frac{2\mu}{\omega_1}\left[\phi'(\omega_1) - \frac{\omega_1}{2}\right]. \tag{17}$$

For convenience, we arbitrarily set $\phi(2) = 1$ so that by Eq. (14a,b) we have

$$\phi'(2) = 1, \qquad \phi''(2) = \frac{\lambda + 2\mu}{2\mu}. \tag{18}$$

From Eqs. (12) and (16), the Piola–Kirchhoff stress (11) has the final form

$$\mathbf{S} = 2\mu\left\{\left[\frac{\phi'(\omega_1)}{\omega_1} - 1\right]\operatorname{cof}\mathbf{F} + \frac{\phi'(\omega_1)}{\omega_1}\mathbf{F}\right\}. \tag{19}$$

A property of this class of materials which we shall use later is that the principal stresses of the Cauchy stress tensor, (τ_1, τ_2), are related to the principal stretches associated with the deformation gradient, (δ_1, δ_2), through

$$\tau_\alpha = 2\mu\left[\frac{\phi'(\omega_1)\delta_\alpha}{J} - 1\right], \quad \alpha = 1, 2. \tag{20}$$

This follows from the Cauchy stress formula

$$\mathbf{T} = 2\mu\left\{\left[\frac{\phi'(\omega_1)}{\omega_1} - 1\right]\mathbf{1} + \frac{\phi'(\omega_1)}{J\omega_1}\mathbf{B}\right\}, \tag{21}$$

(see Eqs. (5) and (19)), the spectral representation

$$\mathbf{B} = \delta_1^2\mathbf{e}_1 \otimes \mathbf{e}_1 + \delta_2^2\mathbf{e}_2 \otimes \mathbf{e}_2, \tag{22}$$

and the identity $\omega_1 = \delta_1 + \delta_2$.

In the next section we comment on some constitutive inequalities that are essential for a harmonic material to be physically sensible.

3. Constitutive inequalities

In addition to the restrictions (18) imposed on the strain energy density ϕ for consistence with the classical linear theory, we also impose restrictions on ϕ that arise from physical requirements concerning the response of the material to elementary experimental observations. For example, let $\delta_1 = \delta_2 = \delta$ in Eq. (20) to obtain

$$\tau_1 = \tau_2 = \tau \equiv 2\mu\left[\frac{\phi'(2\delta)}{\delta} - 1\right]. \tag{23}$$

Under this circumstance, it seems reasonable to assume that $\mathrm{d}\tau/\mathrm{d}\delta > 0$, so that $\phi'(\omega_1)/\omega_1$ is strictly monotone increasing for $0 < \omega_1 < \infty$, i.e.,

$$\frac{\mathrm{d}}{\mathrm{d}\omega_1}\left[\frac{\phi'(\omega_1)}{\omega_1}\right] > 0. \tag{24}$$

Next, consider a rectangle with sides parallel to a rectangular cartesian coordinate system in a state of plane-strain, homogeneous uni-axial tension. The deformation $\mathbf{y}$ is of the form $y_\alpha = \delta_\alpha X_\alpha$, ($\alpha = 1$ or 2, not summed), where δ_1 is the stretch along the axis of tension and δ_2 is obtained from δ_1 by imposing the condition that the lateral sides of the rectangle are traction-free, i.e., $\tau_2(\delta_1, \delta_2) = 0$ in Eq. (20). By requiring that the rectangle gets thinner in the lateral direction while being extended axially, we are lead to the conditions

$$\phi''(\omega_1) > 1, \qquad C \equiv \lim_{\omega_1 \to \infty} \frac{\phi'(\omega_1)}{\omega_1} \geqslant 1. \tag{25}$$

We also expect that for a finite but arbitrarily large stretch δ_1 the rectangle has non-zero width, i.e., $\delta_2 > 0$. This leads to the restrictions

$$\frac{\phi''(\omega_1)}{\omega_1} < 1, \qquad C \leqslant 1, \tag{26}$$

from which, with Eq. (25), follows the explicit upper bound $C = 1$ for $\phi'(\omega_1)/\omega_1$. John (1960) was the first to derive this upper bound. Later, Knowles and Sternberg (1975) argued for this bound and made extensive use of $C = 1$ in the derivation of an asymptotic expression for ϕ that is valid when $\omega_1 \to \infty$. Based upon

these last physical requirements concerning material response, we assume henceforth that the inequalities (25) and (26) hold; in particular, $C = 1$.

Next, the values of ω_1 for which $\phi'(\omega_1) = 0$ play an important role in the analysis of the solutions of equilibrium problems for harmonic materials. For example, if $\phi'(\omega_1) = 0$ then by Eq. (20) the state of stress is a hydrostatic pressure of magnitude 2μ, but yet the stretches need not be equal. Of course, this type of material behavior is not realistic for an isotropic solid and must be avoided. John (1960) used the continuity of ϕ', the conditions (18), and the inequality (24) to show that any solution $\tilde{\omega}_1$ of $\phi'(\tilde{\omega}_1) = 0$ must lie in the range

$$0 \leqslant \tilde{\omega}_1 < 2. \tag{27}$$

On the other hand, it follows from Eq. (20) and the well-known Baker–Ericksen inequality

$$(\tau_1 - \tau_2)(\delta_1 - \delta_2) > 0, \quad \text{for all } \delta_\alpha > 0, \delta_1 \neq \delta_2, \tag{28}$$

that

$$\phi'(\omega_1) > 0, \quad \text{for all } \omega_1 > 0. \tag{29}$$

Clearly, the inequality (29) is incompatible with a zero of $\phi'(\cdot)$ which satisfies $\tilde{\omega}_1 > 0$, and so the harmonic material of Eq. (21) cannot represent an acceptable material behavior for all values of ω_1. Since $\phi'(\omega_1)$ is strictly monotone increasing by Eq. (25a) for $0 < \omega_1 < \infty$, it follows from Eq. (27) that a suitable range of values of ω_1 for which Eq. (21) can possibly be used to represent an acceptable material behavior is given by $\omega_1 > \tilde{\omega}_1$. We shall use this observation to develop a specific constitutive model for a subclass of harmonic materials in Section 4.

4. The bonded punch problem

Here we investigate the behavior of the solution of the plane-strain *bonded punch problem* in the vicinity of the corners of the punch for a subclass of harmonic materials. In this problem, a finite segment of the boundary of a half-plane is forced to undergo a constant rigid normal translation by means of an axially loaded, bonded flat-ended rigid punch. The remainder of the boundary, as well as the points at infinity, are to be free of tractions in such a way that the half-plane is in equilibrium.

4.1. The modified semi-linear material

For the subclass of harmonic materials, we propose a form for the smooth function ϕ' in Eq. (19) that satisfies the inequalities (24)–(26) for all values of $\omega_1 > \tilde{\omega}_1$, where $\tilde{\omega}_1$ is the unique solution of $\phi'(\tilde{\omega}_1) = 0$ which lies in the interval (27). The form is given by

$$\phi'(\omega_1) \equiv \begin{cases} \phi'_s(\omega_1) & \text{if } \omega_1 \leqslant \hat{\omega}_1, \\ \phi'_a(\omega_1) & \text{if } \omega_1 \geqslant \hat{\omega}_1, \end{cases} \tag{30}$$

where ϕ'_s and ϕ'_a are such that $\phi'$and its derivative are continuous at $\omega_1 = \hat{\omega}_1$. The value of $\hat{\omega}_1 > \tilde{\omega}_1$, as well as the functions ϕ'_s and ϕ'_a, are defined below.

To motivate the definition of the function ϕ'_s in Eq. (30) we formally expand ϕ' in a Taylor series about the reference configuration $\omega_1 = 2$, keep only the linear term, and use the conditions (18). Then, we take ϕ'_s to be this affine function, i.e.,

$$\phi'_s(\omega_1) = \frac{1}{2\mu}[(\lambda + 2\mu)\omega_1 - 2(\lambda + \mu)]. \tag{31}$$

It follows from the expressions (30) and (31) and the requirement that $\hat{\omega}_1 > \tilde{\omega}_1$ that $\phi'(\omega_1) = 0$ has the unique solution

$$\tilde{\omega}_1 = 1 + \frac{\lambda}{\lambda + 2\mu}. \tag{32}$$

In passing, the harmonic material characterized by Eqs. (19) and (31) was introduced as the *semi-linear material* by John (1960). This constitutive assumption does not model a generally acceptable material behavior. To see this, we first observe from Eq. (31) that

$$\begin{aligned} \phi_s''(\omega_1) &= \frac{\lambda + 2\mu}{2\mu}, \\ \frac{\phi_s'(\omega_1)}{\omega_1} &= \frac{1}{2\mu}\left[\lambda + 2\mu - \frac{2(\lambda + \mu)}{\omega_1}\right]. \end{aligned} \tag{33}$$

We then recall from Eqs. (25b) and (26b) that $\phi_s'(\omega_1)/\omega_1$ has the explicit upper bound $C = 1$, which, in view of Eq. (33b), requires that we take $\lambda = 0$. But this is in contradiction with the inequality (25a) which, because of Eq. (33a), requires that $\lambda > 0$.

We shall use for ϕ_a' in Eq. (30) the asymptotic constitutive structure proposed by Knowles and Sternberg (1975), which is given by

$$\phi_a'(\omega_1) = \omega_1 - \alpha - \frac{\beta}{\omega_1}, \tag{34}$$

where $0 < \alpha < 1$ and $\beta > 0$. The condition that the material parameter β be positive is necessary for the inequality (25a) to be satisfied. The material parameter α in Eq. (34) has the physical significance of being the limiting value of the transverse stretch δ_2 when a material with such a constitutive structure is subject to a homogeneous uni-axial stretch δ_1, and δ_1 tends to infinity. To see this, we set $\tau_2(\delta_1, \delta_2) = 0$ in Eq. (20), recall Eqs. (30) and (34), and we take the limit of the resulting expression as $\omega_1 \to \infty$.

We call the harmonic material characterized by Eqs. (30), (31), and (34) the *modified semi-linear material*. The material parameters α and β in Eq. (34) are chosen so as to solve the system of equations $\phi_s'(\hat{\omega}_1) = \phi_a'(\hat{\omega}_1), \phi_s''(\hat{\omega}_1) = \phi_a''(\hat{\omega}_1)$, and we shall choose $\hat{\omega}_1 > 2$ so that the modified semi-linear material has the constitutive structure of the semi-linear material in the vicinity of the undistorted state where $\omega_1 \approx 2$. To do this, we first note that

$$\begin{aligned} \alpha &= 1 + (1 - \hat{\omega}_1)\frac{\lambda}{\mu}, \\ \beta &= \hat{\omega}_1^2 \frac{\mu}{2\mu}. \end{aligned} \tag{35}$$

But, because $0 < \alpha < 1$, it follows from Eq. (35a) that $\hat{\omega}_1$ must satisfy

$$2 < \hat{\omega}_1 < 1 + \frac{\mu}{\lambda}, \tag{36}$$

and therefore we are restricted to choose $\lambda < \mu$, which is a limitation on the constitutive structure of the model. In this work we shall take, for illustrative purposes, $\lambda/\mu = 1/4$ and $\hat{\omega}_1 = 4$. The corresponding (linearized) Poisson ratio ν, which is related to the Lamé coefficients λ and μ through $\nu = \lambda/[2(\lambda + \mu)]$, is given by $\nu = 0.10$.

Finally, we use the expressions (19), (30), (31), (34), and (35) to define the Piola–Kirchhoff stress for the modified semi-linear material. It is given by

$$\mathbf{S} = \begin{cases} \left[\lambda - \frac{2(\lambda+\mu)}{\omega_1}\right](\mathbf{F} + \operatorname{cof}\mathbf{F}) + 2\mu\mathbf{F} & \text{for } \omega_1 \leqslant \hat{\omega}_1, \\ -\left[2\mu + \frac{2\lambda(1-\hat{\omega}_1)}{\omega_1} + \lambda\left(\frac{\hat{\omega}_1}{\omega_1}\right)^2\right](\mathbf{F} + \operatorname{cof}\mathbf{F}) + 2\mu\mathbf{F} & \text{for } \omega \geqslant \hat{\omega}_1. \end{cases} \tag{37}$$

The expression (37) is used in Section 4.2 to formulate the bonded punch problem in the nonlinear theory of elasticity.

4.2. Asymptotic results within nonlinear theory

Here we present the mathematical formulation of the bonded punch problem in the nonlinear theory of elasticity and we obtain asymptotic results concerning the solution of this problem in the vicinity of a corner of the punch. For this, we assume that the material governed by Eq. (37) occupies the right half-plane

$$\mathbb{B} = \{(X_1, X_2) | X_1 \geqslant 0, X_2 \in (-\infty, \infty)\} \tag{38}$$

in the undistorted state and that a segment $X_2 \in (-L, L)$ of the boundary of $\mathbb{B}$ is fixed while the remainder of the boundary is traction-free, as shown schematically by the solid lines in Fig. 1.

The bonded punch problem consists of finding a planar deformation field $\mathbf{y}(\mathbf{X}) = \mathbf{X} + \mathbf{u}(\mathbf{X}) : \mathbb{B} \to \mathbb{R}^2$ that satisfies the equation of equilibrium (6) for $\mathbf{S}$ given by Eq. (37) and $\mathbf{F} = \mathbf{1} + \Delta\mathbf{u}$, subject to the boundary conditions

$$\mathbf{u}(\mathbf{X}) = 0, \quad X_1 = 0, \quad X_2 \in (-L, L), \tag{39}$$

$$\mathbf{S}(\mathbf{X})\mathbf{i}_1 = 0, \quad X_1 = 0, \quad |X_2| > L, \tag{40}$$

the condition that the stress field must vanish at infinity,

$$\mathbf{T}(\mathbf{X}) = \mathrm{o}(1) \quad \text{as } |\mathbf{X}| \to \infty \text{ in } \mathbb{B}, \tag{41}$$

and the condition that the displacement field be bounded in the vicinity of the corners of the punch,

$$\mathbf{u}(\mathbf{X}) = \mathrm{O}(1) \quad \text{as } |X \pm L\mathbf{i}_2| \to 0. \tag{42}$$

Recall that the Cauchy stress $\mathbf{T}$ is related to $\mathbf{S}$ through the expression (5). In addition, we require that

$$\int_{-L}^{L} T_{11}(0, X_2)\, \mathrm{d}X_2 = -P, \tag{43}$$

where P is the given punch load – taken positive for an indenting punch, which means that the elastic half-space is displaced into the punch from right to left, as shown schematically by the dashed lines in Fig. 1.

We now turn our attention to the neighborhood of the upper corner of the punch and describe the asymptotic results concerning the behavior of the solution in this neighborhood. Our conclusions here will be compared later with the results of our independent computational scheme. Relative to a translated polar coordinate system (R,Θ) centered at the upper corner $(0,L)$ with Θ measured clockwise negative from the positive X_2-axis, we introduce the semi-circular neighborhood of the corner in the right half-plane

$$\mathbb{N} = \left\{\mathbf{X} = (-R\sin\Theta, R\cos\Theta) \in \mathbb{B} : 0 < R < \overline{R}, -\pi < \Theta < 0\right\}, \tag{44}$$

where $\overline{R}$ is the radius of the semi-circle. The *corner problem* consists of finding the deformation field $\mathbf{y}$: $\mathbb{N} \to \mathbb{R}^2$ that satisfies

$$\operatorname{Div}\mathbf{S} = 0 \quad \text{in } \mathbb{N}, \tag{45}$$

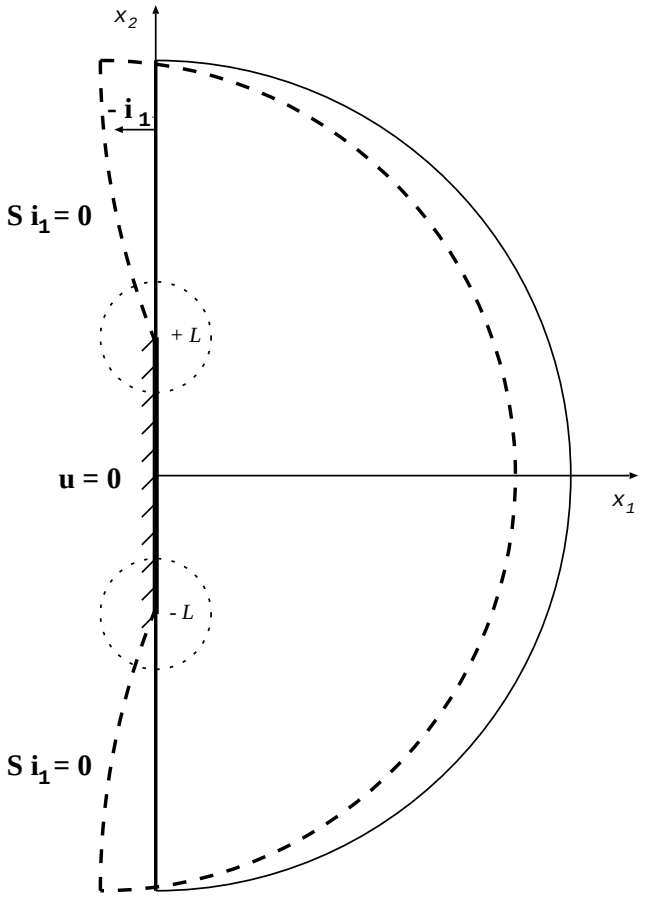

Fig. 1. Two-dimensional version of the bonded punch problem.

where $\mathbf{S}$ is given by Eq. (37) with $\mathbf{F} = \nabla\mathbf{y} = 1 + \nabla\mathbf{u}$, together with prescribed homogeneous displacement and traction boundary conditions on either side of the corner in the interval $R \in (0, \overline{R})$, viz.,

$$\begin{aligned} &\mathbf{u}(R, -\pi) = 0, \\ &(\mathbf{S}\mathbf{e}_\Theta)_{\Theta=0} = 0, \end{aligned} \tag{46}$$

where $\mathbf{e}_R = \mathbf{X}/|\mathbf{X}|$ and $\mathbf{e}_R \cdot \mathbf{e}_\Theta = 0$. Away from the corner, on the circular arc $R = \overline{R}$, we impose

$$\mathbf{y}(\overline{R}, \Theta) = \mathbf{y}^\infty(\Theta) \quad \text{for } -\pi < \Theta < 0, \tag{47}$$

where $\mathbf{y}^\infty$ is the deformation field solution of the bonded punch problem evaluated on $R = \overline{R}$. Since we need to solve the bonded punch problem in $\mathbb{B}$ in order to determine $\mathbf{y}^\infty$ on $R = \overline{R}$, this field is not known a priori. Hence, we can only expect to find a general form of the solution of the corner problem in terms of $\mathbf{y}^\infty$.

While we have not been able to determine a direct asymptotic expansion of the solution $\mathbf{y}$ of the nonlinear partial differential system (45), (46), and (37) in the neighborhood of the corner of the punch, we have managed to show, by following an asymptotic analysis similar to Knowles and Sternberg (1975), that if $\omega_1 \to \infty$ as $R \to 0$ (i.e., if at least one principal stretch becomes unbounded at the corner) then the non-

linear system can be replaced (formally) by a particular linear partial differential system in a sufficiently small neighborhood $\mathbb{N}$. The solution of this *approximate* linear system has the (complex variable) form

$$z(R,\Theta) = R^{1/2}U(\Theta) + RV(\Theta) + o(R), \quad -\pi \leqslant \Theta \leqslant 0, \tag{48}$$

where

$$U(\Theta) = a\cos(\Theta/2), \quad -\pi \leqslant \Theta \leqslant 0, \tag{49}$$

$$V(\Theta) = i\cos\Theta + \frac{2i\alpha a}{3|a|}\left[\cos\Theta + \sin\Theta - ie^{i\Theta/2}\right], \quad -\pi \leqslant \Theta \leqslant 0, \tag{50}$$

and a is a complex constant to be determined using the boundary condition (47). Lacking a proof, we shall assume that the asymptotic behavior of $\mathbf{y}$ is characterized by $\mathbf{z}$ and write

$$\begin{aligned} &y(R,\Theta) = y_1(R,\Theta) + iy_2(R,\Theta) \\ &y(R,\Theta) \sim R^{1/2}U(\Theta) + RV(\Theta) + o(R), \quad -\pi \leqslant \Theta \leqslant 0. \end{aligned} \tag{51}$$

In Section 5 we shall compare the asymptotic expression (51) with our independent numerical solution of a discrete version of the bonded punch problem. We also shall display graphically the behavior of the Jacobian determinant $J = \det\nabla\mathbf{y}$ along the deformed free surface. For the deformed free surface predicted by Eq. (51) with $\Theta = 0$, we have the asymptotic expression

$$J(R,0) \sim \frac{\alpha|a|}{2}R^{-1/2} + o(R^{-1/2}), \tag{52}$$

which is easily obtained from Eq. (51) by employing the well-known expression

$$J = -\Im\left\{\frac{1}{R}\frac{\partial y}{\partial R}\frac{\partial\overline{y}}{\partial\Theta}\right\}. \tag{53}$$

Since we know from Section 4.1 that $\alpha > 0$, it follows from Eq. (52) that $J(R,0) > 0$ in the neighborhood of the upper corner of the punch.

Using the semi-linear constitutive assumption, given by Eq. (19) together with Eq. (31), Aguiar (1998) derived an asymptotic expression for the solution of the Eqs. (45) and (46). This derivation is also based on the assumption that $\omega_1 \to \infty$ as $R \to 0$, and, analogous to Eq. (51), it is given by

$$\hat{y}(R,\Theta) \sim f_1(\Theta)R^{\hat{b}} + R\left[f_2(\Theta) + f_3(\Theta)R^{i\hat{\beta}_2}\right] + o(R), \tag{54}$$

where f_i, $i = 1, 2, 3$, are smooth functions of Θ. The exponent $\hat{b} = \hat{\beta}_1 + i\hat{\beta}_2$ in Eq. (54) is given by

$$\hat{b} = \frac{1}{2} + i\frac{\log\hat{\kappa}}{2\pi}, \tag{55}$$

where the constitutive parameter $\hat{\kappa}$ is defined in terms of the Poisson ratio v as

$$\hat{\kappa} = \frac{1}{1-2v}, \quad 0 < v < 0.5. \tag{56}$$

The imaginary part $\hat{\beta}_2$ of the exponent $\hat{b}$ in Eq. (55) yields an oscillatory behavior for the deformed free surface. Although the corresponding oscillatory part of the asymptotic expression (54) is bounded and smooth up to the boundary, its presence is related to the loss of global and local invertibility of the deformation field.

To characterize the loss of global invertibility, Aguiar (1998) showed that the deformed free surface behaves like a spiral that winds around the corner in the clockwise direction as the corner is approached. Since the punch surface is fixed and the deformation field is continuous up to and including the boundary,

the deformed free surface intersects the punch surface, which is not acceptable. Also, internal material lines in the deformed configuration overlap themselves in the vicinity of the free surface. We shall comment more on this anomalous behavior in the Section 4.3 when we briefly consider a similar anomalous behavior of the deformed free surface within the classical linear theory of elasticity.

To characterize the loss of local invertibility, which corresponds to negative values of the Jacobian determinant $\hat{J}$ associated with the expansion (54), we first use this expansion in Eq. (53) to find that

$$\hat{J}(R,0) \sim \left[\frac{|\hat{a}|}{2(\lambda+2\mu)}\right]^2 R^{-1}\left[1-\mathrm{e}^{2\log\hat{\kappa}}\right] + \mathrm{O}(R^{-1/2}), \tag{57}$$

where $\hat{a}$ is a complex constant to be determined from the boundary condition (47). Since $\hat{\kappa} > 1$ from Eq. (56), it follows from the expression (57) that $\hat{J}(R,0) < 0$ in a small neighborhood of the corner. Aguiar (1998) showed that the negative Jacobian determinant represents mathematically the local eversion of material in the vicinity of the deformed free surface and that both, the negative Jacobian determinant and the local eversion of material, are the manifestation of $C > 1$ in Eqs. (25b) and (33b) for the semi-linear material. Of course, the anomalous behaviors of self-intersection and local inversion of material are not physically acceptable and are only included in this work to illustrate the limitations of the semi-linear constitutive theory.

In the Section 4.3 we consider the solution of the bonded punch problem within the context of classical linear elasticity theory and we present the corresponding asymptotic expression for the deformed configuration of the free surface in the vicinity of the upper corner. Results obtained from this section will be used in Section 5 to validate our computational scheme and to draw comparisons to the results obtained from the nonlinear theory.

4.3. Asymptotic results within linear theory

Here we want to find a planar displacement field $\mathbf{u} : \mathbb{B} \to \mathbb{R}^2$ that satisfies the equation of equilibrium (6) and the conditions (39) through Eq. (43), where $\mathbb{B}$ is the half-plane given by Eq. (38), and both $\mathbf{S}$ and $\mathbf{T}$ are given by the linear constitutive relation

$$\mathbf{S} = \mathbf{T} = \lambda\,\mathrm{Div}\,\mathbf{u} + \mu\left[\nabla\mathbf{u} + (\nabla\mathbf{u})^{\mathrm{T}}\right]. \tag{58}$$

Now, let $u = u_1 + \mathrm{i}u_2$ be the complex representation of the displacement field $\mathbf{u}$ defined in $\mathbb{B}$ and let $v^+(X_2) = \lim_{X_1\to 0} v(X_1,X_2)$ be the limit of a complex function v as X_1 tends to zero from the right side of the punch. The closed form solution for the derivative of the displacement field with respect to X_2 on the unstressed parts of the boundary is

$$\left(\frac{\partial u}{\partial X_2}\right)^+(X_2) = -\frac{(\kappa+1)P}{4\mu\pi}(X_2+L)^{-1/2+\mathrm{i}\gamma}(X_2-L)^{-1/2-\mathrm{i}\gamma}, \tag{59}$$

(Muskhelishvili, 1963) where

$$\kappa = \frac{\lambda+3\mu}{\lambda+\mu} = 3-4\nu, \quad 0<\nu<0.5, \tag{60}$$

for a state of plane strain, with ν being the Poisson ratio, and

$$\gamma = \frac{\log\kappa}{2\pi}. \tag{61}$$

Next, we integrate the expression (59) with respect to X_2, $X_2 > L$, and impose the condition $u(0,L) = 0$. We then find that

$$\tilde{u}(R) \equiv u^+(X_2) = -\frac{(\kappa+1)P}{4\mu\pi b_0}\left(\frac{R}{2L}\right)^{b_0} F(b_0, b_0; b_1; -R/(2L)), \tag{62}$$

where $R = X_2 - L$, F is the Gauss hypergeometric function, and

$$b_n = n + \tfrac{1}{2} - \mathrm{i}\gamma, \quad n = 0, 1, \ldots \tag{63}$$

By expanding F in a Taylor series and substituting the resulting expression in Eq. (62), we obtain the asymptotic expansion

$$\tilde{u}(R) = -\frac{(\kappa+1)P}{4\mu\pi}\left(\frac{R}{2L}\right)^{b_0}\left[\frac{1}{b_0} - \frac{b_0}{b_1}\frac{R}{2L} + \mathrm{O}(R^2)\right] \tag{64}$$

in the vicinity of the upper corner of the punch. The deformed configuration of the free surface is then given by

$$\tilde{y}(R) = R + \tilde{u}(R). \tag{65}$$

Observe from Eqs. (63)–(65) that, for $R \ll 2L$, the first term of $\tilde{u}$ in Eq. (64), which is of the order $\mathrm{O}(R^{1/2})$, dominates and determines the behavior of the deformed free surface. Since the derivative of this term is singular, the region in an infinitesimal neighborhood of the corner will be called the *singular region*. As we move away from the corner and towards the region $R/(2L) = \mathrm{O}(1)$, non-singular terms of the order $\mathrm{O}(R)$ determine the behavior of the deformed free surface. For this reason, the region away from the corner will be called the *far-away region*. When both the singular and non-singular terms are of equal strength, a third region, called the *intermediate region*, exists between the singular and the far-away regions. It turns out that interesting structure develops in the intermediate region not only within the linear theory but also in the nonlinear case presented in Section 4.2. Details about these structures will be given in Section 5 when we display graphically our asymptotic and computational results for the deformed free surface within both the nonlinear (i.e., semi-linear and modified semi-linear) theory (recall Eqs. (51) and (54)) and the linear theory.

Now, the imaginary part of the exponent b_0, given by $-\gamma$ in Eq. (63), yields an oscillatory behavior for the position of the deformed free surface as given by Eqs. (64) and (65) in the vicinity of the upper corner. To investigate this behavior further, we observe that the complex function

$$\left(\frac{R}{2L}\right)^{-\mathrm{i}\gamma} = \mathrm{e}^{-\mathrm{i}\gamma\log[R/(2L)]}, \qquad \mathrm{e}^{-2\pi/\gamma} \leqslant \frac{R}{2L} < 1, \tag{66}$$

corresponds to a unit circle in the complex plane. Using Eqs. (60) and (61), we also observe that with one anti-clockwise revolution on this circle the value of R decreases from $R = 2L$ to $R = 2L\mathrm{e}^{-2\pi/\gamma}$. Since $0 < \nu < 0.5$ for compressible materials commonly used in engineering, we have from Eq. (60) that $1 < \kappa < 3$ and, with Eq. (61), that $0 < \mathrm{e}^{-2\pi/\gamma} < \mathrm{e}^{-(2\pi)^2/\log 3} \approx 2.5 \times 10^{-16}$. This range for $\mathrm{e}^{-2\pi/\gamma}$ becomes important later in the visualization of the deformed free surface, because, as we move from the far-away region to the singular region, different *zoom-ins* of the free surface at different scale distances are necessary to visualize the behavior of the free surface in the vicinity of the corner.

The expression (66) now shows that the complex function

$$\left(\frac{R}{2L}\right)^{1/2}\mathrm{e}^{-\mathrm{i}\gamma\log[R/(2L)]}, \quad \mathrm{e}^{-2\pi/\gamma} \leqslant \frac{R}{2L} < 1, \tag{67}$$

corresponds to one revolution of a spiral with focus at the origin $R = 0$. Hence, it follows from the first term of the asymptotic expansion (64) that the free surface winds around the upper corner of the punch in the anti-clockwise direction as R varies in the singular region. To characterize the interpenetration of matter in

the vicinity of this corner, we only need to recall that the displacement field is continuous up to and including the boundary and vanishes on $\Theta = -\pi$.

Performing a similar analysis on the asymptotic expression (54) when $\Theta = 0$ we find that, for a semi-linear material, the term

$$\left(\frac{R}{2L}\right)^{1/2} e^{i\hat{\beta}_2 \log R}, \quad e^{-2\pi/\hat{\beta}_2} \leqslant \frac{R}{2L} < 1, \tag{68}$$

where $\hat{\beta}_2$ is the imaginary part of Eq. (55), corresponds to one revolution of a spiral with focus at the origin $R = 0$. Since $\hat{\kappa} > 1$ in Eq. (56), $\hat{\beta}_2 > 0$ in Eq. (55) and the spiral winds around the corner in the clockwise direction as $R \to 0$. Since the displacement field is continuous up to and including the boundary and vanishes on $\Theta = -\pi$, the free surface intersects the punch surface, which characterizes interpenetration of matter.

Observe that the exponent $\hat{b}$ in Eq. (55) and the constitutive parameter $\hat{\kappa}$ in Eq. (56) are analogous to, respectively, b_n in Eq. (63) for $n = 0$ and κ in Eq. (60). Notice that the parameter $\hat{\kappa}$ is sensitive to the choice of ν and changes significantly the spiral-like behavior of the free surface from the corresponding solution of the linear problem. In the linear theory, as the Poisson ratio ν varies from 0 to 0.5, the free surface varies from a configuration with infinite oscillations to one with non-oscillatory behavior; for the semi-linear material, it varies from a configuration with non-oscillatory behavior to one with infinite oscillations.

We emphasize that no such anomalous oscillatory behavior is predicted by the modified semi-linear material, because the exponents of R in the expression (51) have no imaginary parts.

Similar to our work of Section 4.2, we find, with the help of the expressions (53) and (64), that

$$\tilde{J}(R) \equiv J(R,0) \sim \tilde{J}_1(R)\tilde{J}_2(R) + O(R^{-1/2}), \tag{69}$$

where

$$\tilde{J}_1(R) = (\kappa - 1) + 2\cos\left(2\gamma \log\left(\frac{2L}{R}\right)\right), \tag{70}$$

$$\tilde{J}_2(R) = \frac{(\kappa+1)P^2}{(4\mu\pi)^2 2LR} \tag{71}$$

(Aguiar, 1998). Since $1 < \kappa < 3$, it follows from Eqs. (69)–(71) that $\tilde{J}(R)$ oscillates between positive and negative values as the corner is approached.

In the Section 5 we introduce the variational equations used in our computational scheme, which is based on the numerical method presented by Aguiar and Fosdick (2000), and we compute a numerical solution to the bonded punch problem within nonlinear elasticity. We then compare our numerical solution with results obtained from the asymptotic expressions (51) together with Eqs. (49) and (50) in the neighborhood of the upper corner of the punch.

5. Asymptotic versus computational results

Our computational procedure is based on a classical Galerkin formulation of the bonded punch problem. It applies to both the linear and nonlinear theories. In the nonlinear theory, we first define a 1-parameter family of kinematically admissible deformations by

$$\mathbb{S}_\lambda \equiv \left\{\mathbf{y}_\lambda \in \mathbb{W}^{1,2}(\mathbb{B}) : \mathbf{y}_\lambda(\mathbf{X}) = \mathbf{X} + \lambda[\bar{\mathbf{y}}(\mathbf{X}) - \mathbf{X}] \quad \text{for } \mathbf{X} \in \Gamma_y\right\}, \tag{72}$$

where $\lambda \in \mathbb{R}$. We then use the definition (72) together with a continuation technique described in Aguiar and Fosdick (2000) to construct a continuous *path of states* through the solution of a problem at $\lambda = 1$,

starting from the trivial solution $\mathbf{y}_0 = \mathbf{X}$ at $\lambda = 0$. A path of states is the set of all $(y_\lambda, \lambda) \in \mathbb{S}_\lambda \times [0,1]$ that satisfy the variational equation

$$h^*(\mathbf{y}_\lambda, \lambda) = a(\mathbf{y}_\lambda, \mathbf{v}) - \lambda\langle \bar{\mathbf{s}}, \mathbf{v}\rangle = 0, \quad \forall \mathbf{v} \in \mathbb{W}_0^{1,2}(\mathbb{B}), \tag{73}$$

where, for harmonic materials,

$$a(\mathbf{y}_\lambda, \mathbf{v}) \equiv \int_{\mathbb{B}} \frac{\phi'(\omega_{1\lambda})}{\omega_{1\lambda}} (\mathbf{F}_\lambda + \operatorname{cof} \mathbf{F}_\lambda) \cdot \nabla \mathbf{v} \, \mathrm{d}A \tag{74}$$

and

$$\langle \bar{\mathbf{s}}, \mathbf{v}\rangle \equiv \int_{\Gamma_s} \bar{\mathbf{s}} \cdot \mathbf{v} \, \mathrm{d}S. \tag{75}$$

Here, $\mathbb{W}_0^{1,2}(\mathbb{B})$ denotes the set of all functions in $\mathbb{W}^{1,2}(\mathbb{B})$ which vanish on the part $\Gamma_y \subset \partial\mathbb{B}$; these are referred to as kinematically admissible variations. Also, recall from Eq. (10) that $(\omega_{1\lambda})^2 = |\mathbf{F}_\lambda|^2 + 2 \det \mathbf{F}_\lambda$ where $\mathbf{F}_\lambda = \nabla \mathbf{y}_\lambda$, and from Eqs. (7) and (8) that Γ_y and Γ_s are the regular parts of the boundary $\partial\mathbb{B}$ where the deformation $\bar{\mathbf{y}}$ and the traction $\bar{\mathbf{s}}$ are imposed, respectively.

The variational problem in nonlinear elastostatics that corresponds to the mixed problem (6)–(8), and (19) consists of finding a continuous path of states $(\mathbf{y}_\lambda, \lambda) \in \mathbb{S}_\lambda \times [0,1]$ so that $h^*(\mathbf{y}_\lambda, \lambda) = 0$ in Eq. (73). We solved the corresponding discrete nonlinear problem by means of the computational scheme described in Aguiar and Fosdick (2000).

The domain of discretization $\mathbb{B}_\mathrm{h} \subset \mathbb{B}$ is finite and composed of isoparametric elements $P2$. In particular, we use a fan of these elements in the vicinity of the upper corner. We find that this finite element mesh allows for a better interpretation of our computations in the vicinity of the corner and also it yields an improvement over computations which use rectangular elements. The points of $\mathbb{B}$ at infinity are replaced by points on the boundary of $\mathbb{B}_\mathrm{h}$ whose distances from the origin are at least two orders of magnitude greater than the width $2L$ of the punch surface.

In Fig. 2 we show both material lines and the free surface shape close to the upper corner of the bonded punch in the undistorted state. Observe the high level of mesh refinement in the vicinity of the corner when compared to points away from the corner. The thick white line represents the *punch surface* and the black line represents the *scale distance* in terms of the width of the punch.

On the right side, the *gray scale* represents values of the Jacobian determinant $J = \det \mathbf{F}$. Based on this gray scale, we will compare the values of J on the free surface obtained from the asymptotic representations (52) of the modified semi-linear constitutive assumption, Eq. (57) of the semi-linear constitutive assumption, and Eqs. (69)–(71) of the classical linear theory, with the corresponding values obtained from our computational scheme. Values of J greater than $+2$ are represented by the white color, while values of J smaller than -2 are represented by the black color. In particular, notice that both the material lines and the free surface shape are gray in the undistorted state. We shall track both the positive and negative values of the determinant in the computations because this illustrates more clearly the structure of the solution in the neighborhood of a singular corner point. While an everywhere positive determinant is acceptable, the existence of negative values is related to self-intersection and keynotes a deficiency in the constitutive model. A plot of the indenting punch load P versus the horizontal displacement U imposed on the boundary of $\mathbb{B}_\mathrm{h}$ is shown at the upper right corner.

When we hold fixed the number of elements in the radial direction and increase the number of elements in the polar angular direction, we observe the following in both the linear and nonlinear cases:

- For the same horizontal displacement U imposed on the boundary of $\mathbb{B}_\mathrm{h}$, the deformation field converges everywhere in the domain, including the vicinity of the corner;
- The traction-free conditions are closely satisfied everywhere on the boundary of the discrete domain $\mathbb{B}_\mathrm{h}$.

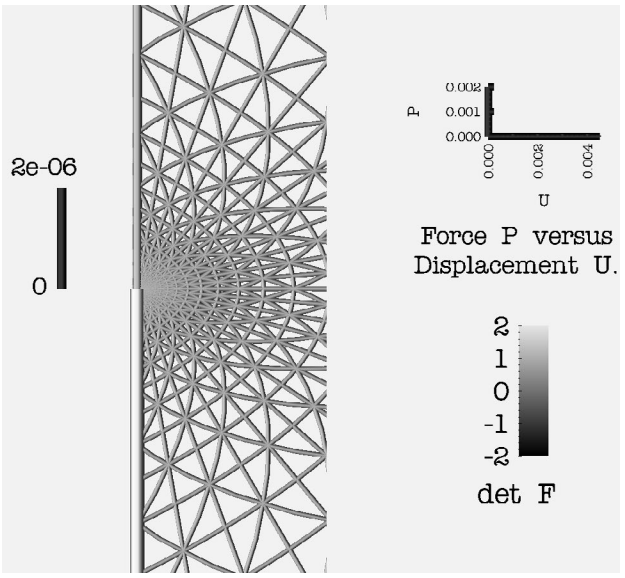

Fig. 2. Neighborhood of the upper corner of the punch.

We increase the number of elements in the radial direction by considering a sequence of discretizations that starts with a *coarse mesh* for which the closest node to the upper corner is at a distance of the order $O(10^{-11}L)$. The other meshes are obtained from the coarse mesh by both doubling the number of nodes in the R-direction and then applying a nonlinear function to the distribution of nodes in the R-direction in order to increase the density of nodes in the vicinity of the corner. By following this procedure we arrive at the fifth and final discretization of the sequence with the closest node to the upper corner being at a distance of the order $O(10^{-19}L)$.

When we increase the number of elements in the radial direction and consider the discrete nonlinear problem, the numerical scheme converges for a moderate horizontal displacement U imposed on the boundary of $\mathbb{B}_h$. When U exceeds a cut-off value U_c, the continuation technique described in Aguiar and Fosdick (2000) fails to produce an accurate solution to this problem. The loss of accuracy seems to be related to the presence of a material instability that occurs in the vicinity of a particular point on the deformed free surface. At this point, which is at a distance of the order $O(10^{-6}L)$ from the upper corner, we have observed that $\omega_1 \to \tilde{\omega}_1$ as $U \to U_c$. We will comment more on this later in this section.

In the linear case, the displacement field is proportional to the punch load P (see Eq. (62)). Thus, it suffices to calculate the numerical solution of the discrete linear problem once for a given horizontal displacement on the boundary of $\mathbb{B}_h$, say $\tilde{U}$, and then multiply this solution by the factor $U/\tilde{U}$ in order to obtain a numerical solution of the discrete linear problem for an arbitrary value of U.

5.1. Linear theory

We now describe graphically our asymptotic and computational results from linear theory. Recall from Section 4.3 that the solution of the linear bonded punch problem is well-known and can be found in the classical literature (e.g., Milne-Thomson (1968) and Muskhelishvili (1963)). Thus, we use the solution of the linear problem to check and authenticate our computational scheme in the vicinity of the corners

of the punch. We also compare this solution later to the solution of the nonlinear bonded punch problem.

Again, our computations are based on the finite element method described in Aguiar and Fosdick (2000). We first consider the deformation of the free surface in the vicinity of the upper corner, and then show the corresponding behavior of internal material lines and the free surface shape in the neighborhood of this corner. Finally, we zoom in further and show the free surface shape at small scale distance, order $O(10^{-10}L)$, from the corner of the punch, where we recall that $2L$ is the width of the punch surface. At smaller scales the pattern is similar as it follows a logarithmic spiral behavior.

Consider the free surface shape near, order $O(10^{-5}L)$, the upper corner of the punch as predicted by both the asymptotic solution (64) and the numerical solution of the discrete linear problem. In Fig. 3 we show a sequence of frames that illustrate the self-intersecting material behavior in the neighborhood of this corner for increasing values of the punch displacement U. In Fig. 3a we see the undistorted state of the punch in the vicinity of the upper corner. In Fig. 3b the free surface shape is indicated by two lines; a thick line obtained from the asymptotic solution and a thin line obtained from the numerical computations. Approximation errors in both the asymptotic and the computational procedures account for the difference between the two solutions which, according to the scale distance, is small. Both predictions show that material is drawn under the punch and that as the corner is approached, $\det \mathbf{F}$ is first negative and then positive again. The transition region between negative and positive values is very thin and is not perceptible in this image. For a moderately large load, Fig. 3c shows that the numerical solution becomes cusp-like. Now it is possible to observe a smooth transition region between positive and negative values of $\det \mathbf{F}$. Notice also the good agreement between the asymptotic and computational results with respect to both the surface shape and the values of $\det \mathbf{F}$. In Fig. 3d the cusp becomes looped and the free surface intersects itself. The good agreement between the asymptotic and computational results is more visible. In Fig. 3e we change the scale from 2 to $8 \times 10^{-5}L$ to better illustrate the intersection of the free surface with the punch surface. The good agreement between the asymptotic and computational results is observed once again. In the last figure of the sequence, Fig. 3f, we show that the intersection of the free surface with the punch surface persists as the load increases.

Next, in Fig. 4, we show a sequence of frames that illustrates the behavior of both internal material lines and free surface shape near, order $O(10^{-5}L)$, the upper corner of the punch as predicted by our numerical computations. This sequence of frames corresponds to the sequence shown in Fig. 3, and both were obtained with a coarser level of mesh refinement than shown in Fig. 2. This mesh refinement suffices to produce very accurate results at low computational cost. In Fig. 4a we show the flat, rigid, bonded punch (thick white line), the free surface (thick gray line), and the material lines (thin gray lines) of the half-plane at zero punch displacement. In Fig. 4b material is drawn under the punch and the free surface intersects internal material lines of the half-plane. This anomalous intersection characterizes eversion of material in the vicinity of the free surface; notice from the shades of dark and light gray that $\det \mathbf{F}$ also changes sign near these places of eversion. In Fig. 4c the cusp-like shape of the free surface for a moderately large load is clearly intersecting internal material lines of the elastic half-plane and, again, this intersection is related to a nearby change of sign of $\det \mathbf{F}$. In Fig. 4d the cusp becomes looped and the free surface intersects itself inside the elastic region. In Fig. 4e we change the scale from 2 to $8 \times 10^{-5}L$ to show the intersection of both the material lines and the free surface with the punch surface. In the last figure of the sequence, Fig. 4f, we see that the intersection of both the material lines and the free surface with the punch surface persists.

In the sequence of Fig. 5, we show the asymptotic behavior (i.e., Eqs. (64) and (65)) and the numerical solution of the free surface shape at small scale distance, order $O(10^{-10}L)$, from the upper corner of the punch. Both predictions are indistinguishable at this scale distance. The undistorted state is shown in Fig. 5a and b we see the free surface shape for a small punch displacement and we show that $\det \mathbf{F}$ alternates between positive and negative values as the corner is approached. Fig. 5c is the same as Fig. 3c but at five orders of magnitude closer to the corner. The cusp is very far away at this magnification and cannot be

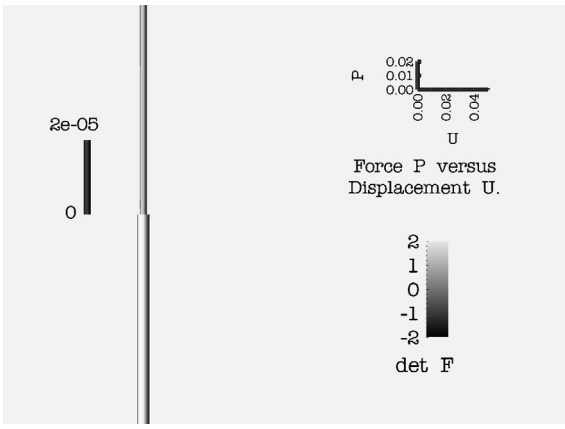

a) Reference configuration

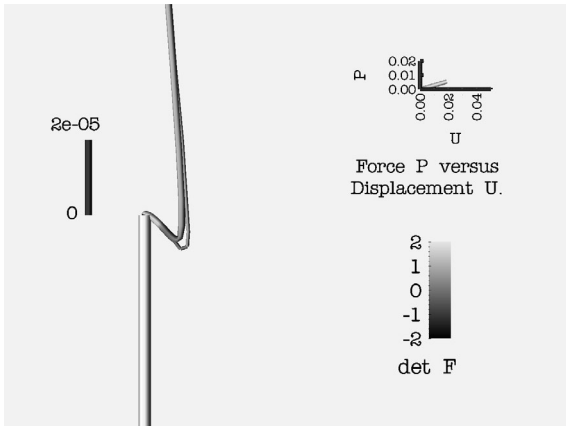

b) Material is drawn under the punch

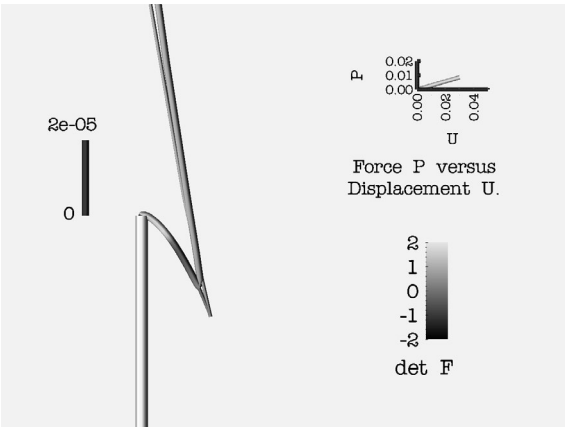

c) Cusp-like shape

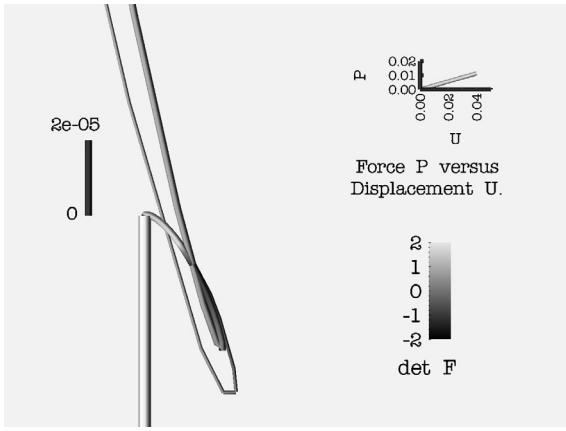

d) Free surface becomes looped

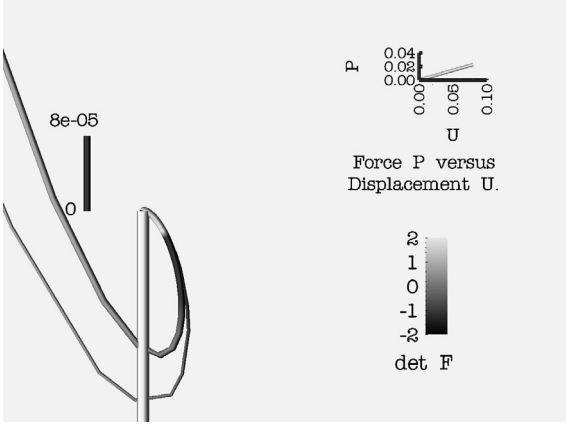

e) Free surface intersects the punch

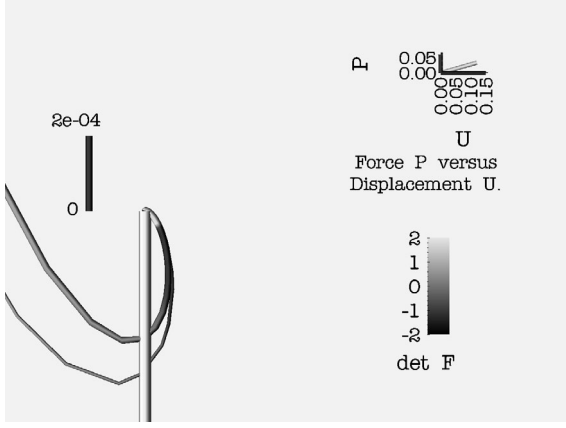

f) Last image of the series

Fig. 3. (Classical linear theory) Anomalous behavior of the free surface shape for increasing normal punch displacements.

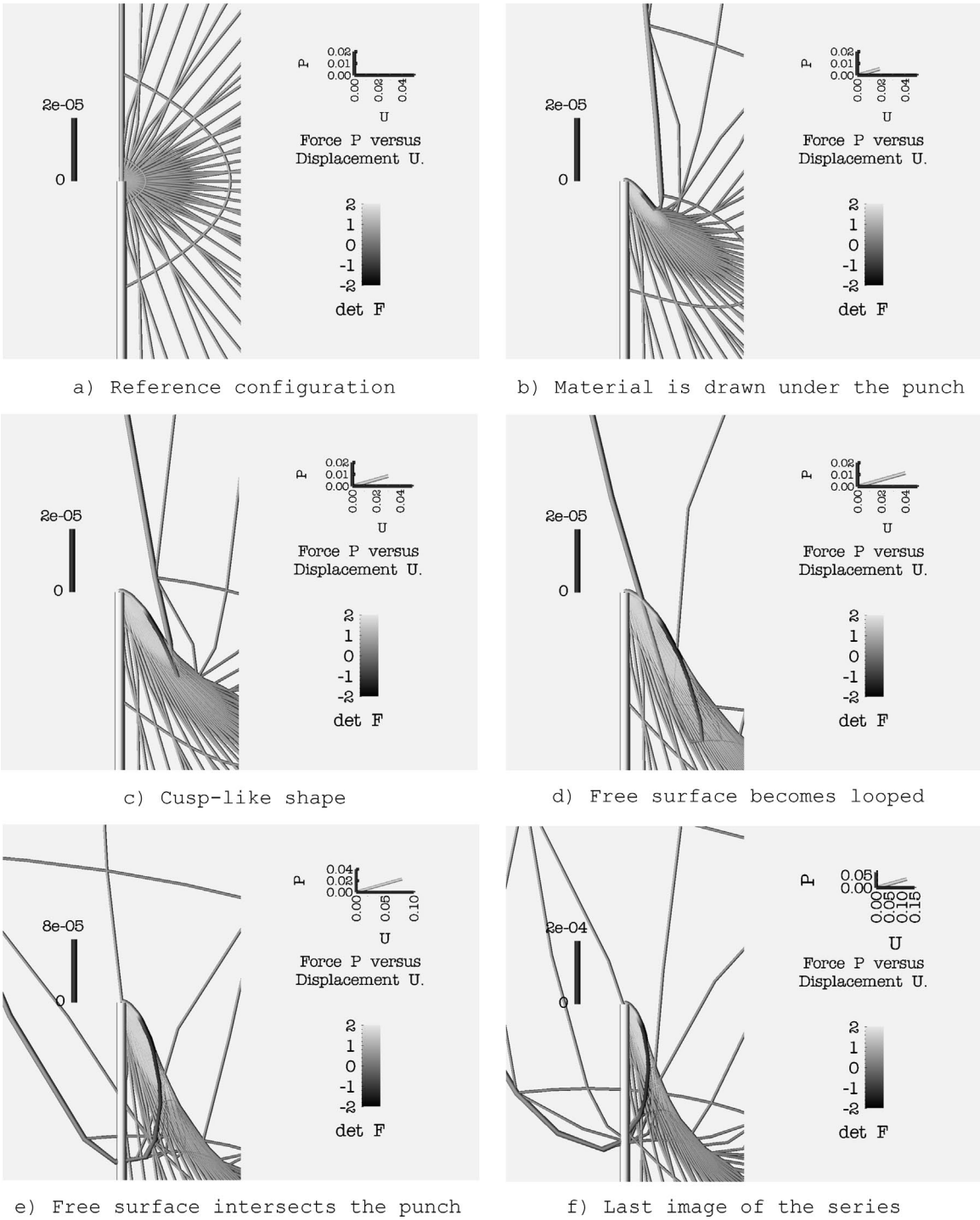

Fig. 4. (Classical linear theory) The behavior of both material lines and free surface shape for increasing normal punch displacements.

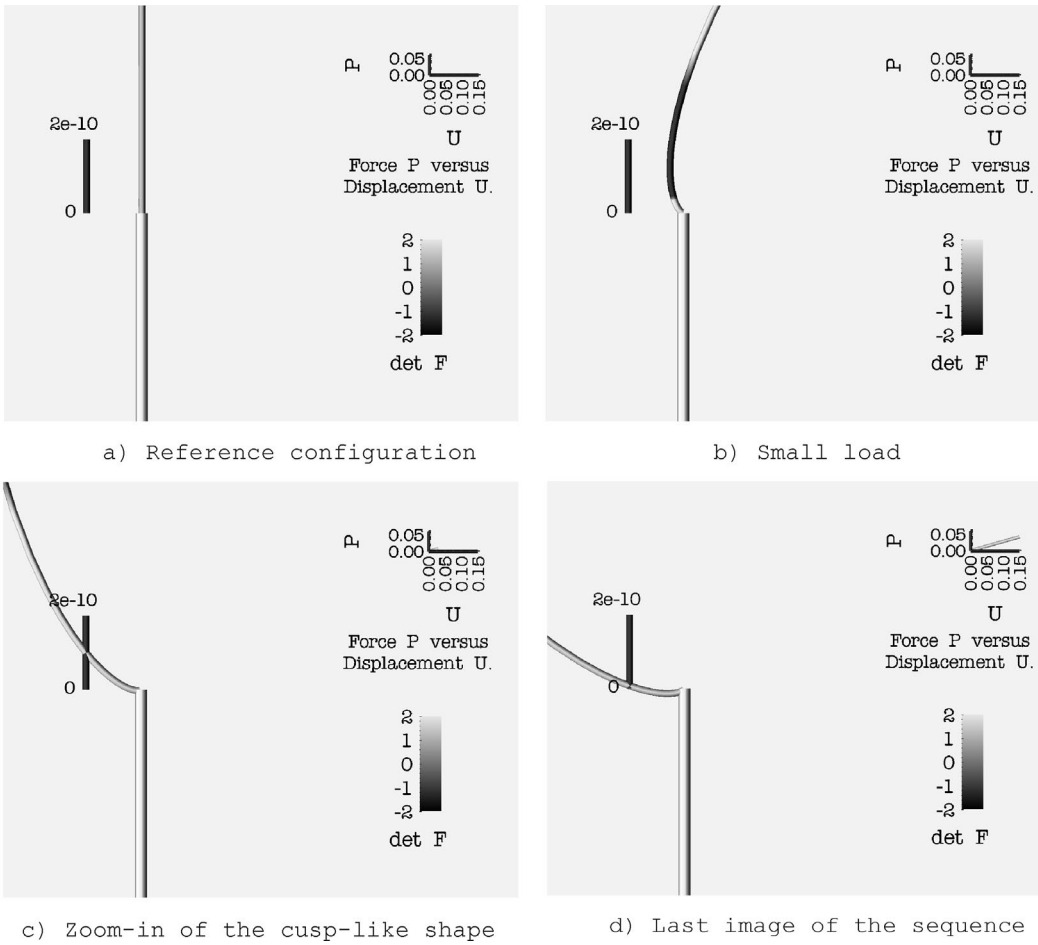

Fig. 5. (Classical linear theory) The behavior of the free surface shape at small scale distance, order $O(10^{-10}L)$, from the corner of the punch.

seen, but a spiral-like shape at the corner can be inferred by comparing these figures. Fig. 5d indicates that the spiral-like behavior of the free surface persists at a larger load.

Based upon the asymptotic expression (64) together with Eq. (65), and the exposition above, we identify the following three regions of the linear elastic behavior in the vicinity of the upper corner of the punch:

- A *singular region* consisting of points very close to the corner. In this region, $R \ll 2L$, the first term of $\tilde{u}$ in Eq. (64) dominates and, with Eq. (65), it determines the placement of the deformed free surface. The deformed free surface has a spiral-like shape and the Jacobian determinant oscillates between positive and negative values as the corner is approached.
- A *far-away region* consisting of points sufficiently (but not arbitrarily) far from the corner, so that the first term in Eq. (65), i.e., R, and the higher order terms in Eq. (64), $O(R^{\beta_1})$ for $\beta_1 \geqslant 3/2$, dominate and determine the behavior of the deformed free surface. In the far-away region, the deformed free surface has the shape depicted by the dashed line in Fig. 1, which is on the left side of the punch surface.
- An *intermediate region* consisting of points not contained in the first two regions. In this region, both singular and non-singular terms determine the placement of the deformed free surface and predict that

this surface must be on the right side of the punch surface. The cusp-like shape of the free surface shown in Fig. 3c originates from points belonging to the intermediate region.

In summary, as the corner is approached, the deformed free surface is first on the left side of the punch surface for points in the far-away region, then it comes to the right side of this surface for points in the intermediate region, and finally it winds around the upper corner of the punch in a counter-clockwise direction for points in the singular region. Although the spiral-like behavior of the deformed free surface in the singular region is not acceptable, the non-monotone behavior observed in the other two regions is possible. As we shall see later in this section, a similar non-monotone behavior is also predicted by the modified semi-linear theory.

5.2. Nonlinear theory

Here, we interpret graphically our asymptotic and computational results for the solution of the bonded punch problem within the nonlinear theory of elasticity for the modified semi-linear constitutive assumption (37).

First, we check our computational scheme for its ability to approximate well the stress field in the vicinity of the free surface. For this, let us consider a small material square with sides of length ε and let one side lie on the undistorted free surface boundary $\Theta = 0$ while the remainder of the square cuts orthogonal to the free surface and lies within $\mathbb{B}_h$. Since the outer unit normal field to $\mathbf{y}(\mathbb{B}_h)$ on the deformed free surface is a principal direction of the Cauchy stress $\mathbf{T}$, we expect that, for $\mathbf{y}$ sufficiently smooth and for a sufficiently small $\varepsilon > 0$, the planar state of stress for this material square is nearly one of uni-axial tension (or compression) in its distorted state. We have numerically computed the Cauchy stress field in $\mathbf{y}(\mathbb{B}_h)$ and we have found that the state of stress in the vicinity of the deformed free surface is indeed close to a state of uni-axial tension (or compression) for every sufficiently small material square situated along the free surface as described above.

In passing, we recall from Section 3 that while the inequalities (25) were motivated by our expectation that a rectangle thins transversely as it is stretched axially, the inequalities (26) were motivated by our further expectation that for a finite but arbitrarily large stretch δ_1 the rectangle maintains a non-zero width. The existence of a stretch δ_1 for which the width of the rectangle vanishes is then a manifestation of the inequality $C > 1$. In fact, when $C > 1$ the lateral sides of a sufficiently stretched rectangle can be made to reverse their relative positions and the Jacobian determinant will become negative. The change of sign of the Jacobian determinant is then associated with the local eversion of material for a rectangle under uni-axial tension. This fact about uni-axial tension together with our analysis of the state of stress in the vicinity of the deformed free surface lead to the conclusion that a negative Jacobian determinant represents a local eversion of material in this vicinity and that both are the manifestation of setting $C > 1$ in the constitutive equation for harmonic materials.

We have numerically computed the sum of the stretches ω_1 in $\mathbf{y}(\mathbb{B}_h)$ and we have found that ω_1 is very large in the vicinity of the deformed free surface and very close to the punch corner. Hence, we have independently verified (apart from the asymptotic results in Section 4.2) that self-intersection should not be expected in the case of the modified semi-linear material because $C = 1$ in that case, and it should be expected in the case of the semi-linear material because there we have $C = 1 + \lambda/(2\mu) > 1$.

We now turn our attention to the asymptotic and computational results for the solution of the bonded punch problem using the modified semi-linear constitutive assumption (37). Recall from Section 4.2 that the second-order approximation of the (complex) deformation field y is given by the first two terms of the asymptotic expansion in Eq. (51) together with both Eqs. (49) and (50). This approximation is fully determined with the exception of the complex constant a. To estimate a, we first found the best curve fitting to a set of points on the deformed free surface as predicted by our numerical computations. The derivative of

the complex function that corresponds to this curve fitting has a square-root singularity in a small neighborhood of the corner. The factor multiplying the term $R^{1/2}$ in this complex function was then taken as the constant a.

In Fig. 6 we show the form of the free surface according to both the second-order asymptotic formula of Eq. (51) together with Eqs. (49) and (50) and the computational predictions at the scale distance $O(10^{-10}L)$. The two graphs lie on top of one another, especially in the region of large values of $\det \mathbf{F}$. In Fig. 6c and d we show both the free surface shape and the internal material lines as determined from our computational finite element method for the same scale distance $O(10^{-10}L)$. The computations show the existence of a singular region in a neighborhood of the corner, for which large spatial changes of deformation occur and for which $\det \mathbf{F}$ is indeed positive.

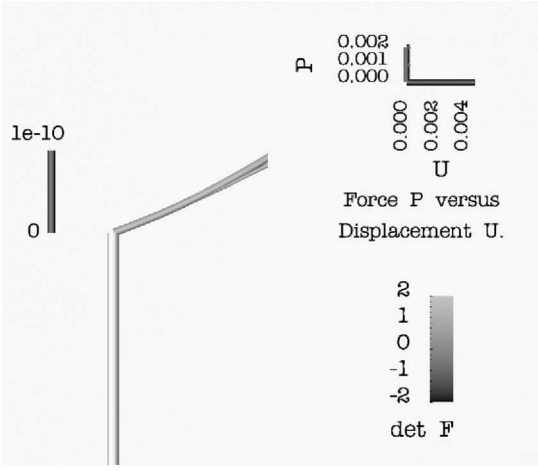

a) Free Surface Shape - Small P

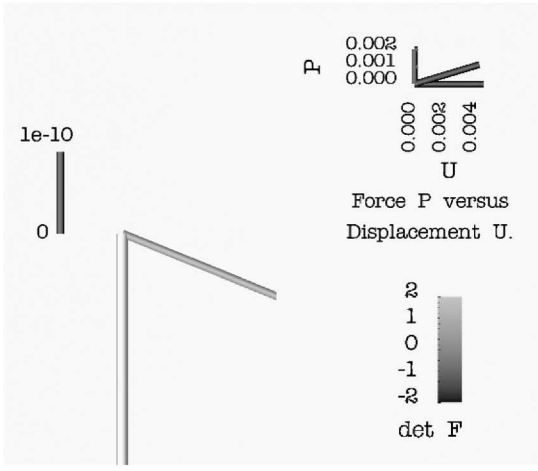

b) Free Surface Shape - Larger P

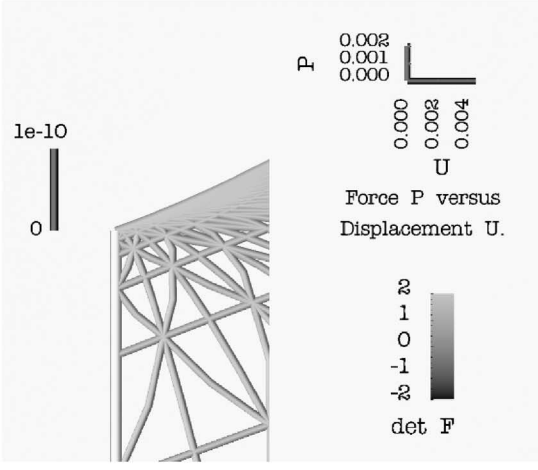

c) Material Lines - Small P

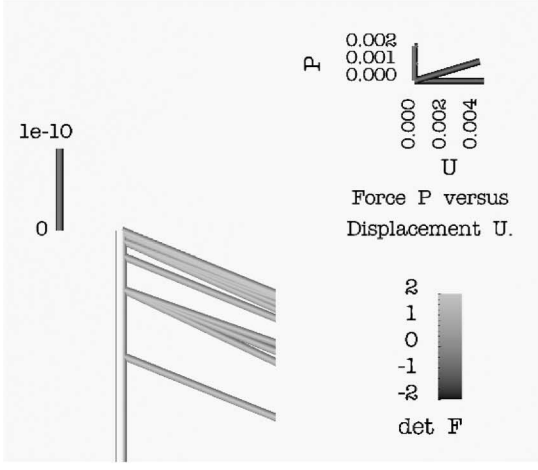

d) Material Lines - Larger P

Fig. 6. (Modified semi-linear theory) Material lines and free surface shape at scale distance $O(10^{-10}L)$.

In Fig. 7 we reduce the magnification by four orders so that an intermediate region of the corner can be observed. In Fig. 7a, we see that the second-order asymptotic approximation of the free surface, represented by the thick line, agrees well with our finite element computations, represented by the thin line, in the singular region, characterized here as the region where $\det \mathbf{F} > 2$. But, as we move away from the corner, our computations show a sharp change of curvature of the free surface in the intermediate region. In fact, this sharp change of curvature occurs at the first point in the intermediate region where ω_1 approaches $\tilde{\omega}_1$, where $\tilde{\omega}_1$ satisfies $\phi'(\tilde{\omega}_1) = 0$ and is given by Eq. (32). The significance of this is that the equations of

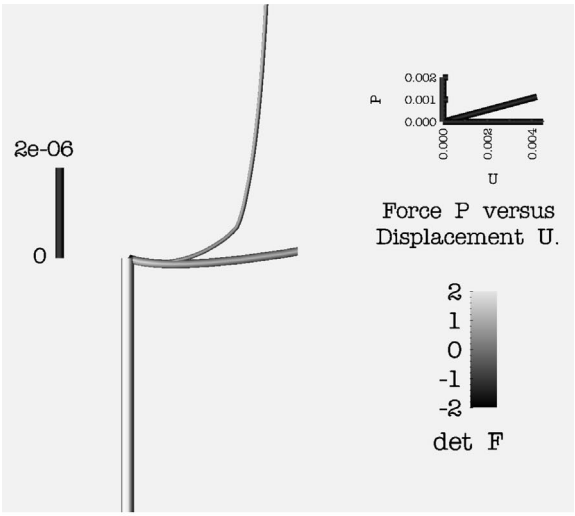

a) Free Surface Shape Large P

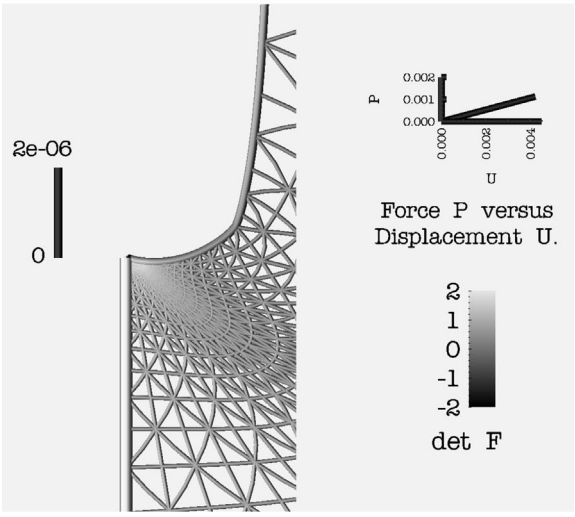

b) Material Lines Large P

Fig. 7. (Modified semi-linear theory) Material lines and free surface shape at scale distance $O(10^{-6}L)$.

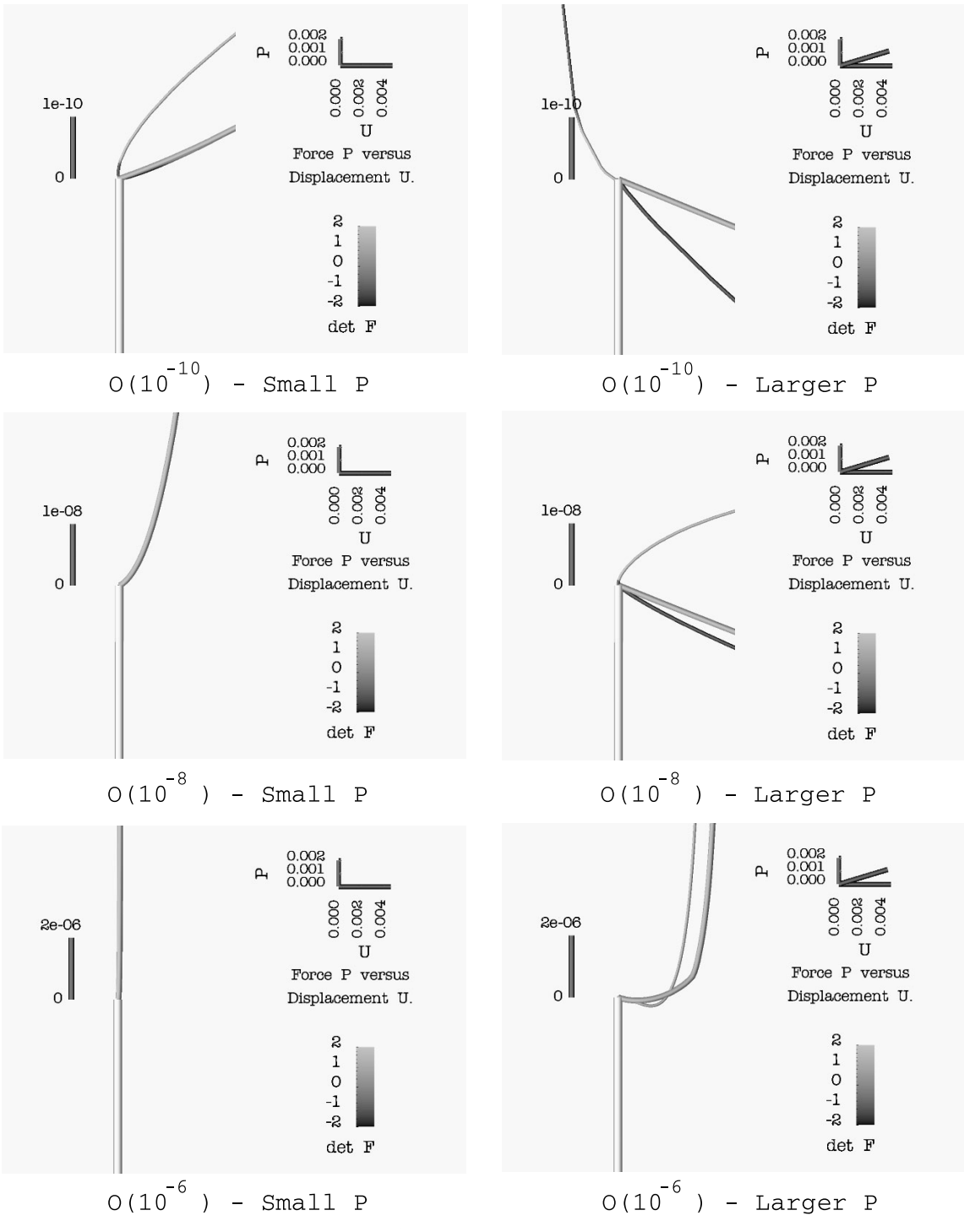

Fig. 8. Linear versus nonlinear (semi-linear and modified semi-linear constitutive assumptions) asymptotic solution.

equilibrium suffer a loss of strong ellipticity at such a point, as Knowles and Sternberg (1977) have shown. Note that the Jacobian determinant $\det \mathbf{F}$ is strictly positive in the vicinity of this point. In this intermediate region the modified semi-linear constitutive assumption (37) actually corresponds to the semi-linear form and it predicts possible behavior. Of course, in the singular region neighboring the corner the semi-linear constitutive assumption is not an acceptable model for studying the material behavior and we introduced the modified semi-linear form for that reason.

In Fig. 8 we compare the form of the free surface as predicted by our finite element computations for the linear, the semi-linear, and modified semi-linear theories. To do so, we have chosen the same Lamé coefficients λ and μ in these theories, so that the modified semi-linear theory reduces to the linear theory for small displacement gradients. Note that we have included a calculation for the semi-linear constitutive assumption, as well, even though we know that it fails to represent reasonable material behavior in the singular region neighboring the corner. The free surfaces for the linear, semi-linear, and modified semi-linear materials are represented by thin, medium, and thick lines, respectively. At the scale distance of order $O(10^{-10}L)$ and for large P, the shapes of the deformed free surfaces differ considerably. Also, the Jacobian determinant $\det \mathbf{F}$ is large ($|\det \mathbf{F}| > 2$) for all three materials. It changes sign for the linear material, is negative for the semi-linear material, and is positive for the modified semi-linear material. Clearly, a negative Jacobian determinant, which corresponds to interpenetration of matter, is not physically acceptable, and so both the linear and semi-linear materials are not reasonable models for studying the behavior of an elastic material in the vicinity of a corner. Nevertheless, the deformed free surfaces, while very different in the so-called singular region very close to the corner, become nearly parallel to each other as we move away from the corner into the far-away region where $\det \mathbf{F} \approx 1$. In particular, the deformed free surfaces for the nonlinear materials (i.e., the semi-linear and modified semi-linear) become indistinguishable. Finally, we observe that while physical intuition might suggest that the free surface should deform to the left of the indenting punch surface in Fig. 8, the deformed free surface for all three models is seen to be on the right side of the punch surface when viewed at a scale distance of order $O(10^{-6}L)$ and for large P.

6. Conclusion

We have compared asymptotic approximations and computational predictions obtained from the solution of singular problems in elasticity theory. We have concentrated our attention on the singular structure of the bonded punch problem in the three cases of linear, semi-linear, and modified semi-linear theories. In these cases, the computational results are in good agreement with the asymptotic approximations.

We have identified three regions with different characteristic behaviors in these theories.

- In the *singular region* neighboring the corner of the punch, these theories predict a square root singularity for the stress field. The linear and the semi-linear materials predict an oscillatory behavior of the corresponding deformation fields, which yields spiral-like behaviors for the deformed free surfaces, and negative Jacobian determinants, which are related to a spurious self-intersection anomaly. The orientations of the spirals and the material constants are, however, different. The modified semi-linear material does not share the anomalous oscillatory behavior and it satisfies $\det \mathbf{F} > 0$ everywhere in the vicinity of the corners of the punch.
- In the *far-away region*, these theories predict similar regular behavior. In particular, the free surface shapes for the semi-linear and modified semi-linear materials are indistinguishable in this region.
- In the *intermediate region*, these theories predict that the deformed free surface is depressed lower than the flat punch surface, itself. This curious non-monotonic behavior of the free surface is analogous to the non-monotonic behavior of the deformed free surface of the compressed bonded block near the end plattens as

mentioned in Section 1. The modified semi-linear theory predicts a sharp change of curvature of the free surface for a sufficiently large punch load. We believe that this sharp change is related to the onset of a material instability.

Acknowledgements

The authors wish to acknowledge the CNPq (Brazilian National Council of Research), proc. # 200110/90-0, the NSF under grant DMS-9531925, and the University of Minnesota Supercomputing Institute for their support of this research.

References

Aguiar, A.R., 1998. Singular problems in elasticity, Ph.D. Thesis, University of Minnesota.

Aguiar, A.R., Fosdick, R.L., 2000. A singular problem in incompressible nonlinear elastostatics. Mathematical Models and Methods in the Applied Sciences 10 (8), 1–27.

Aravas, N., Sharma, S.M., 1991. An elastoplastic analysis of the interface crack with contact zones. Journal of the Mechanics and Physics of Solids 39 (3), 311–344.

Bogy, D.B., 1971. Two edge-bonded elastic wedges of different materials and wedge angles under surface tractions. ASME Journal of Applied Mechanics 38, 377–386.

Carroll, M.M., 1988. Finite strain solutions in compressible isotropic elasticity. Journal of Elasticity 20, 65–92.

Comninou, M., 1977. The interface crack. ASME Journal of Applied Mechanics 44, 631–636.

Comninou, M., 1978. The interface crack in a shear field. ASME Journal of Applied Mechanics 45, 287–290.

Comninou, M., Schmueser, D., 1979. The interface crack in a combined tension-compression and shear field. ASME Journal of Applied Mechanics 46, 345–358.

Dauge, M., 1988. Elliptic boundary value problems on corner domains – smoothness and asymptotics of solutions. Lecture Notes in Mathematics, Springer, Berlin, p. 1341.

Fosdick, R.L., Schuler, K.W., 1969. On Ericksen's problem for plane deformations with uniform transverse stretch. International Journal of Engineering Science 7, 217–233.

Grisvard, P., 1985. Elliptic problems in non-smooth domains. Monographs and Studies in Mathematics, Pitman, London, p. 24.

Grisvard, P., 1986. Problèmes aux limites dans les polygones – mode d'emploi, E. D. F. Bulletin de la Direction des Etudes et Recherches, Série C. Mathématiques, Informatiques 1, 21–59.

Grisvard, P., 1992. Singularities in boundary value problems, RMA 22. Collection Recherches en Mathématiques Appliquées, Masson, Paris.

Isherwood, D.A., Ogden, R.W., 1977. Towards the solution of finite plane-strain problems for compressible elastic solids. International Journal of Solids and Structures 13, 105–123.

John, F., 1960. Plane strain problems for a perfectly elastic material of harmonic type. Communications on Pure and Applied Mathematics, XIII, 239–296.

Kondrat'ev, V.A., 1967. Boundary problems for elliptic equations in domains with conical or angular points. Transactions of the Moscow Mathematical Society 16, 226–313.

Kondrat'ev, V.A., Oleinik, O.A., 1983. Boundary-value problems for partial differential equations in non-smooth domains. Russian Mathematical Surveys 38 (2), 1–86.

Knowles, J.K., Sternberg, E., 1975. On the singularity induced by certain mixed boundary conditions in linearized and nonlinear elastostatics. International Journal of Solids and Structures 11, 1173–1201.

Knowles, J.K., Sternberg, E., 1977. On the failure of ellipticity of the equations for finite elastostatic plane strain. Archive for Rational Mechanics and Analysis 63, 321–336.

Leguillon, D., Sanchez-Palência, E., 1987. Computation of singular solutions in elliptic problems and elasticity. RMA 5, Collection Recherches en Mathématiques Appliquées, Masson, Paris.

Milne-Thomson, L.M., 1968. Plane elastic systems. Springer, Berlin.

Muskhelishvili, N.I., 1963. Some basic problems of the mathematical theory of elasticity. P. Wolters-Noordhoff, Groningen.

Ogden, R.W., 1977. Inequalities associated with the inversion of elastic stress-deformation relations and their implications. Mathematical Proceedings of the Cambridge Philosophical Society 81, 313–324.

Reitich, F., 1991. Singular solutions of a transmission problem in plane linear elasticity for wedge-shaped regions. Numerische Mathematik 59, 179–216.

Rice, J.R., Sih, G.C., 1965. Plane problems of cracks in dissimilar media. Journal of Applied Mechanics 32, ASME Journal of Applied Mechanics 87 (Series E), 418–423.

Steigmann, D.J., Pipkin, A.C., 1988. Stability of harmonic materials in plane strain. Quarterly of Applied Mathematics XLVI, 559–568.

Williams, M.L., 1959. The stresses around a fault or crack in dissimilar media. Bulletin of the Seismological Society of America 49, 199–204.